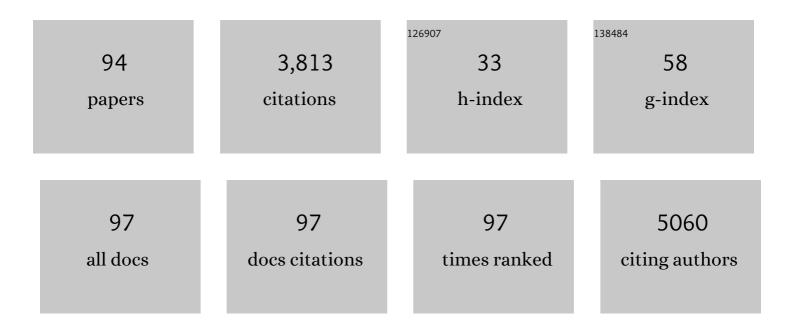


## List of Publications by Year in descending order

Source: https://exaly.com/author-pdf/2904073/publications.pdf Version: 2024-02-01



ZIROLI

#	Article	lF	CITATIONS
1	A PBPK model recapitulates early kinetics of anti-PEG antibody-mediated clearance of PEG-liposomes. Journal of Controlled Release, 2022, 343, 518-527.	9.9	5
2	The Synthesis and Initial Evaluation of MerTK Targeted PET Agents. Molecules, 2022, 27, 1460.	3.8	0
3	Arene radiofluorination enabled by photoredox-mediated halide interconversion. Nature Chemistry, 2022, 14, 216-223.	13.6	25
4	Development of <sup>18</sup> F-Labeled Vinyl Sulfone–PSMAi Conjugates as New PET Agents for Prostate Cancer Imaging. Molecular Pharmaceutics, 2022, 19, 720-727.	4.6	3
5	Synthesis and Evaluation of <sup>18</sup> F-Labeled Boramino Acids as Potential New Positron Emission Tomography Agents for Cancer Management. Molecular Pharmaceutics, 2022, , .	4.6	2
6	Radiodynamic therapy with CsI(na)@MgO nanoparticles and 5-aminolevulinic acid. Journal of Nanobiotechnology, 2022, 20, .	9.1	3
7	FAPâ€Targeted Photodynamic Therapy Mediated by Ferritin Nanoparticles Elicits an Immune Response against Cancer Cells and Cancer Associated Fibroblasts. Advanced Functional Materials, 2021, 31, 2007017.	14.9	37
8	Ultrasmall Gd@Cdots as a radiosensitizing agent for non-small cell lung cancer. Nanoscale, 2021, 13, 9252-9263.	5.6	11
9	Phototherapy and multimodal imaging of cancers based on perfluorocarbon nanomaterials. Journal of Materials Chemistry B, 2021, 9, 6751-6769.	5.8	15
10	Assessment of 18F-PBR-111 in the Cuprizone Mouse Model of Multiple Sclerosis. Diagnostics, 2021, 11, 786.	2.6	1
11	Development of Novel 18F-PET Agents for Tumor Hypoxia Imaging. Journal of Medicinal Chemistry, 2021, 64, 5593-5602.	6.4	9
12	Enabling <i>In Vivo</i> Photocatalytic Activation of Rapid Bioorthogonal Chemistry by Repurposing Silicon-Rhodamine Fluorophores as Cytocompatible Far-Red Photocatalysts. Journal of the American Chemical Society, 2021, 143, 10793-10803.	13.7	47
13	18F-PEG1-Vinyl Sulfone-Labeled Red Blood Cells as Positron Emission Tomography Agent to Image Intra-Abdominal Bleeding. Frontiers in Medicine, 2021, 8, 646862.	2.6	2
14	Image-guided selection of Gd@C-dots as sensitizers to improve radiotherapy of non-small cell lung cancer. Journal of Nanobiotechnology, 2021, 19, 284.	9.1	16
15	High MW polyethylene glycol prolongs circulation of pegloticase in mice with anti-PEG antibodies. Journal of Controlled Release, 2021, 338, 804-812.	9.9	8
16	Potassium Iodide Nanoparticles Enhance Radiotherapy against Breast Cancer by Exploiting the Sodium-Iodide Symporter. ACS Nano, 2021, 15, 17401-17411.	14.6	7
17	Bioequivalence assessment of high-capacity polymeric micelle nanoformulation of paclitaxel and Abraxane® in rodent and non-human primate models using a stable isotope tracer assay. Biomaterials, 2021, 278, 121140.	11.4	15
18	A Novel PET Probe for Brown Adipose Tissue Imaging in Rodents. Molecular Imaging and Biology, 2020, 22, 675-684.	2.6	8

#	Article	IF	CITATIONS
19	Escalating morphine dosing in HIV-1 Tat transgenic mice with sustained Tat exposure reveals an allostatic shift in neuroinflammatory regulation accompanied by increased neuroprotective non-endocannabinoid lipid signaling molecules and amino acids. Journal of Neuroinflammation, 2020, 17, 345.	7.2	13
20	RXH-Reactive <sup>18</sup> F-Vinyl Sulfones as Versatile Agents for PET Probe Construction. Bioconjugate Chemistry, 2020, 31, 2482-2487.	3.6	10
21	19F- and 18F-arene deoxyfluorination via organic photoredox-catalysed polarity-reversed nucleophilic aromatic substitution. Nature Catalysis, 2020, 3, 734-742.	34.4	53
22	Ultrathin gold nanowires to enhance radiation therapy. Journal of Nanobiotechnology, 2020, 18, 131.	9.1	15
23	Barium tungstate nanoparticles to enhance radiation therapy against cancer. Nanomedicine: Nanotechnology, Biology, and Medicine, 2020, 28, 102230.	3.3	7
24	Human beige adipocytes for drug discovery and cell therapy in metabolic diseases. Nature Communications, 2020, 11, 2758.	12.8	40
25	β-Arrestin-Biased Allosteric Modulator of NTSR1 Selectively Attenuates Addictive Behaviors. Cell, 2020, 181, 1364-1379.e14.	28.9	74
26	Tetrazine-TCO Ligation: A Potential Simple Approach to Improve Tumor Uptake through Enhanced Blood Circulation. Bioconjugate Chemistry, 2020, 31, 1795-1803.	3.6	9
27	Improving Tumorâ€ŧoâ€Background Contrast through Hydrophilic Tetrazines: The Construction of 18 Fâ€Labeled PET Agents Targeting Nonsmall Cell Lung Carcinoma. Chemistry - A European Journal, 2020, 26, 4690-4694.	3.3	9
28	Comparative evaluation of 68Ga-labelled TATEs: the impact of chelators on imaging. EJNMMI Research, 2020, 10, 36.	2.5	8
29	Deletion of Topoisomerase 1 in excitatory neurons causes genomic instability and early onset neurodegeneration. Nature Communications, 2020, 11, 1962.	12.8	24
30	Direct Radiofluorination of Arene C–H Bonds via Photoredox Catalysis Using a Peroxide as the Terminal Oxidant. Organic Letters, 2020, 22, 7971-7975.	4.6	18
31	High intratumoral tryptophan metabolism is a poor predictor of response to pembrolizumab (pembro) in metastatic melanoma (MM): Results from a prospective trial using baseline C11-labeled alpha-methyl tryptophan (C11-AMT) PET imaging for response prediction Journal of Clinical Oncology, 2020, 38, 3556-3556.	1.6	3
32	Evaluation of neurotensin receptor 1 as potential biomarker for prostate cancer theranostic use. European Journal of Nuclear Medicine and Molecular Imaging, 2019, 46, 2199-2207.	6.4	11
33	NaCl Nanoparticles as a Cancer Therapeutic. Advanced Materials, 2019, 31, e1904058.	21.0	74
34	Hydrophilic <sup>18</sup> F-labeled <i>trans</i> -5-oxocene (oxoTCO) for efficient construction of PET agents with improved tumor-to-background ratios in neurotensin receptor (NTR) imaging. Chemical Communications, 2019, 55, 2485-2488.	4.1	23
35	Perfluorocarbon-based O <sub>2</sub> nanocarrier for efficient photodynamic therapy. Journal of Materials Chemistry B, 2019, 7, 1116-1123.	5.8	53
36	Direct arene C–H fluorination with <sup>18</sup> F <sup>â^'</sup> via organic photoredox catalysis. Science, 2019, 364, 1170-1174.	12.6	120

#	Article	IF	CITATIONS
37	Synthesis and initial evaluation of radioactive 5-I-α-methyl-tryptophan: a Trp based agent targeting IDO-1. MedChemComm, 2019, 10, 814-816.	3.4	2
38	Development of Bispecific NT-PSMA Heterodimer for Prostate Cancer Imaging: A Potential Approach to Address Tumor Heterogeneity. Bioconjugate Chemistry, 2019, 30, 1314-1322.	3.6	8
39	Clinical Application of 18F-AlF-NOTA-Octreotide PET/CT in Combination With 18F-FDG PET/CT for Imaging Neuroendocrine Neoplasms. Clinical Nuclear Medicine, 2019, 44, 452-458.	1.3	47
40	A Novel 18F-Labeling Method for the Synthesis of [18F]-Piperidine-Containing Ligands as Potential PET Radiotracers for σ Receptors. Synlett, 2018, 29, 410-414.	1.8	2
41	P-glycoprotein targeted photodynamic therapy of chemoresistant tumors using recombinant Fab fragment conjugates. Biomaterials Science, 2018, 6, 3063-3074.	5.4	11
42	Nanoparticle‣aden Macrophages for Tumorâ€Tropic Drug Delivery. Advanced Materials, 2018, 30, e1805557.	21.0	143
43	P-glycoprotein targeted and near-infrared light-guided depletion of chemoresistant tumors. Journal of Controlled Release, 2018, 286, 289-300.	9.9	18
44	Development of [18F]AlF-NOTA-NT as PET Agents of Neurotensin Receptor-1 Positive Pancreatic Cancer. Molecular Pharmaceutics, 2018, 15, 3093-3100.	4.6	25
45	The efficiency of <sup>18</sup> F labelling of a prostate specific membrane antigen ligand <i>via</i> strain-promoted azide–alkyne reaction: reaction speed <i>versus</i> hydrophilicity. Chemical Communications, 2018, 54, 7810-7813.	4.1	9
46	Silver-promoted (radio)fluorination of unsaturated carbamates via a radical process. Chemical Communications, 2017, 53, 3497-3500.	4.1	49
47	Evaluation of neurotensin receptor 1 as a potential imaging target in pancreatic ductal adenocarcinoma. Amino Acids, 2017, 49, 1325-1335.	2.7	28
48	Preparation of [18F]-NHC-BF3 conjugates and their applications in PET imaging. RSC Advances, 2017, 7, 17748-17751.	3.6	9
49	Protein Nanocage Mediated Fibroblast-Activation Protein Targeted Photoimmunotherapy To Enhance Cytotoxic T Cell Infiltration and Tumor Control. Nano Letters, 2017, 17, 862-869.	9.1	167
50	lmaging Neurotensin Receptor in Prostate Cancer With <sup>64</sup> Cu-Labeled Neurotensin Analogs. Molecular Imaging, 2017, 16, 153601211771136.	1.4	17
51	Molecular Imaging of P-glycoprotein in Chemoresistant Tumors Using a Dual-Modality PET/Fluorescence Probe. Molecular Pharmaceutics, 2017, 14, 3391-3398.	4.6	18
52	LiGa <sub>5</sub> O <sub>8</sub> :Cr-based theranostic nanoparticles for imaging-guided X-ray induced photodynamic therapy of deep-seated tumors. Materials Horizons, 2017, 4, 1092-1101.	12.2	128
53	Radiofluorination of a NHC–PF <sub>5</sub> adduct: toward new probes for <sup>18</sup> F PET imaging. Chemical Communications, 2017, 53, 8657-8659.	4.1	17
54	Synthesis of 5-[ <sup>18</sup> F]Fluoro-α-methyl Tryptophan: New Trp Based PET Agents. Theranostics, 2017, 7, 1524-1530.	10.0	34

#	Article	IF	CITATIONS
55	Conformationally Strained <i>trans-</i> Cyclooctene (sTCO) Enables the Rapid Construction of <sup>18</sup> F-PET Probes via Tetrazine Ligation. Theranostics, 2016, 6, 887-895.	10.0	56
56	Spatial Disassociation of Disrupted Functional Connectivity for the Default Mode Network in Patients with End-Stage Renal Disease. PLoS ONE, 2016, 11, e0161392.	2.5	13
57	X-Ray Induced Photodynamic Therapy: A Combination of Radiotherapy and Photodynamic Therapy. Theranostics, 2016, 6, 2295-2305.	10.0	171
58	A potent immunotoxin targeting fibroblast activation protein for treatment of breast cancer in mice. International Journal of Cancer, 2016, 138, 1013-1023.	5.1	91
59	Synthesis and Evaluation of [ <sup>18</sup> F]â€Ammonium BODIPY Dyes as Potential Positron Emission Tomography Agents for Myocardial Perfusion Imaging. Chemistry - A European Journal, 2016, 22, 12122-12129.	3.3	30
60	Biodistribution and Radiation Dosimetry of the Enterobacteriaceae-Specific Imaging Probe [18F]Fluorodeoxysorbitol Determined by PET/CT in Healthy Human Volunteers. Molecular Imaging and Biology, 2016, 18, 782-787.	2.6	31
61	Infection Imaging With 18F-FDS and First-in-Human Evaluation. Nuclear Medicine and Biology, 2016, 43, 206-214.	0.6	51
62	A high capacity polymeric micelle of paclitaxel: Implication of high dose drug therapy to safety and inÂvivo anti-cancer activity. Biomaterials, 2016, 101, 296-309.	11.4	151
63	Red Blood Cellâ€Facilitated Photodynamic Therapy for Cancer Treatment. Advanced Functional Materials, 2016, 26, 1757-1768.	14.9	167
64	Synthesis and in vivo stability studies of [ <sup>18</sup> F]-zwitterionic phosphonium aryltrifluoroborate/indomethacin conjugates. RSC Advances, 2016, 6, 23126-23133.	3.6	11
65	Small-Animal PET Imaging of Pancreatic Cancer Xenografts Using a <sup>64</sup> Cu-Labeled Monoclonal Antibody, MAb159. Journal of Nuclear Medicine, 2015, 56, 908-913.	5.0	17
66	Improved Metabolic Stability for <sup>18</sup> F PET Probes Rapidly Constructed via Tetrazine <i>trans</i> -Cyclooctene Ligation. Bioconjugate Chemistry, 2015, 26, 435-442.	3.6	36
67	Synthesis and Evaluation of <sup>64</sup> Cu-DOTA-NT-Cy5.5 as a Dual-Modality PET/Fluorescence Probe to Image Neurotensin Receptor-Positive Tumor. Molecular Pharmaceutics, 2015, 12, 3054-3061.	4.6	25
68	[ <sup>18</sup> F]–NHC–BF <sub>3</sub> adducts as water stable radio-prosthetic groups for PET imaging. Chemical Communications, 2015, 51, 12439-12442.	4.1	34
69	PET Imaging of Dll4 Expression in Glioblastoma and Colorectal Cancer Xenografts Using <sup>64</sup> Cu-Labeled Monoclonal Antibody 61B. Molecular Pharmaceutics, 2015, 12, 3527-3534.	4.6	7
70	Matching Chelators to Radiometals for Positron Emission Tomography Imaging- Guided Targeted Drug Delivery. Current Drug Targets, 2015, 16, 610-624.	2.1	8
71	Development of Multi-Functional Chelators Based on Sarcophagine Cages. Molecules, 2014, 19, 4246-4255.	3.8	18
72	<sup>64</sup> Cu Labeled Sarcophagine Exendin-4 for MicroPET Imaging of Glucagon like Peptide-1 Receptor Expression. Theranostics, 2014, 4, 770-777.	10.0	36

#	Article	IF	CITATIONS
73	Facile Preparation of a Thiol-Reactive <sup>18</sup> F-Labeling Agent and Synthesis of <sup>18</sup> F-DEG-VS-NT for PET Imaging of a Neurotensin Receptor–Positive Tumor. Journal of Nuclear Medicine, 2014, 55, 1178-1184.	5.0	29
74	Efficient synthesis of fluorescent-PET probes based on [18F]BODIPY dye. Chemical Communications, 2014, 50, 7371.	4.1	48
75	Integrin α2β1 targeted GdVO4:Eu ultrathin nanosheet for multimodal PET/MR imaging. Biomaterials, 2014, 35, 8649-8658.	11.4	45
76	The synthesis of lanthanide-doped GdVO <sub>4</sub> ultrathin nanosheets with great optical and paramagnetic properties for FRET biodetection and in vivo MR imaging. Journal of Materials Chemistry B, 2014, 2, 3998-4007.	5.8	23
77	Evaluation of 18F-labeled BODIPY dye as potential PET agents for myocardial perfusion imaging. Nuclear Medicine and Biology, 2014, 41, 120-126.	0.6	26
78	Development and Evaluation of <sup>18</sup> F-TTCO-Cys <sup>40</sup> -Exendin-4: A PET Probe for Imaging Transplanted Islets. Journal of Nuclear Medicine, 2013, 54, 244-251.	5.0	98
79	Efficient <sup>18</sup> F Labeling of Cysteine-Containing Peptides and Proteins Using Tetrazine– <i>Trans</i> -Cyclooctene Ligation. Molecular Imaging, 2013, 12, 7290.2012.00013.	1.4	43
80	Lewis Acid-Assisted Isotopic <sup>18</sup> F- <sup>19</sup> F Exchange in BODIPY Dyes: Facile Generation of Positron Emission Tomography/Fluorescence Dual Modality Agents for Tumor Imaging. Theranostics, 2013, 3, 181-189.	10.0	83
81	Quantum Dot Conjugates for Optical Imaging of Cancer. , 2012, , 483-517.		0
82	Harvesting 18F-fluoride ions in water via direct 18F–19F isotopic exchange: radiofluorination of zwitterionic aryltrifluoroborates and in vivo stability studies. MedChemComm, 2012, 3, 1305.	3.4	50
83	Rapid aqueous [18F]-labeling of a bodipy dye for positron emission tomography/fluorescence dual modality imaging. Chemical Communications, 2011, 47, 9324.	4.1	97
84	Biological Stability Evaluation of the α2β1 Receptor Imaging Agents: Diamsar and DOTA Conjugated DGEA Peptide. Bioconjugate Chemistry, 2011, 22, 256-263.	3.6	13
85	In Vivo Imaging of Transplanted Islets with <sup>64</sup> Cu-DO3A-VS-Cys <sup>40</sup> -Exendin-4 by Targeting GLP-1 Receptor. Bioconjugate Chemistry, 2011, 22, 1587-1594.	3.6	80
86	Automated synthesis of 2′-deoxy-2′-[18F]fluoro-5-methyl-1-β-d-arabinofuranosyluracil ([18F]-FMAU) using a one reactor radiosynthesis module. Nuclear Medicine and Biology, 2011, 38, 201-206.	0.6	22
87	Improved Synthesis of 2-deoxy-2-[18F]fluoro-5-Methyl-1-β-DArabinofuranosyluracil ([18F]FMAU). Current Radiopharmaceuticals, 2011, 4, 24-30.	0.8	2
88	Trackable and Targeted Phage as Positron Emission Tomography (PET) Agent for Cancer Imaging. Theranostics, 2011, 1, 371-380.	10.0	30
89	Novel &#x03B1; <sub>2</sub> &#x03B2; <sub>1</sub> Integrin-Targeted Peptide Probes for Prostate Cancer Imaging. Molecular Imaging, 2011, 10, 7290.2010.00044.	1.4	22
90	Tetrazine-trans-cyclooctene ligation for the rapid construction of integrin αvβ3 targeted PET tracer based on a cyclic RGD peptide. Bioorganic and Medicinal Chemistry Letters, 2011, 21, 5011-5014.	2.2	93

#	Article	IF	CITATIONS
91	Design, synthesis and validation of integrin $\hat{I}\pm 2\hat{I}^21$ -targeted probe for microPET imaging of prostate cancer. European Journal of Nuclear Medicine and Molecular Imaging, 2011, 38, 1313-1322.	6.4	22
92	<i>In Vivo</i> Near-Infrared Fluorescence Imaging of Integrin α <sub>2</sub> 1² <sub>1</sub> in Prostate Cancer with Cell-Penetrating-Peptide–Conjugated DGEA Probe. Journal of Nuclear Medicine, 2011, 52, 1979-1986.	5.0	33
93	Radiopharmaceutical chemistry for positron emission tomography. Advanced Drug Delivery Reviews, 2010, 62, 1031-1051.	13.7	174
94	Tetrazine–trans-cyclooctene ligation for the rapid construction of 18F labeled probes. Chemical Communications, 2010, 46, 8043.	4.1	172